forum acusticum 2026
8-12 September · Graz, Austria

A Surface-Based Geometrical Acoustics Algorithm Inc. Diffraction

Jonathan A. Hargreaves[1]

[1]*Acoustics Research Centre, University of Salford, Salford, United Kingdom*

Abstract

Raytracing is an established method for computing the late-time part of room impulse responses, but it has the drawback that only very crude Monte Carlo models of boundary scattering and diffraction are possible to include without it losing its attractive computational cost scaling. This happens because higher-resolution models of these processes output multiple child rays for every parent ray received, making the number of rays grow with reflection order. An emerging solution is so-called 'Surface-Based' Geometrical Acoustics (SBGA). Here the distribution of rays arriving at a boundary is mapped onto a predefined set of spatial elements and angular interpolation functions, producing a vector of coefficients. Re-radiation of subsequent reflections is then a matrix multiplication, with the steady state being solvable via a Neumann series. Since rays only ever propagate one reflection order before being collected, diffraction and scattering processes that cause them to multiply can be included without issue. In this paper an approach to efficiently represent edge diffraction in such algorithms is presented. It involves discretising the sound energy arriving and departing an edge versus angle and representing the diffraction via a matrix multiplication relating these coefficients. Indicative results demonstrate the approach.

Keywords: diffraction, room acoustics

1. Introduction

For the last 30+ years [1], Geometrical Acoustics (GA) algorithms have been the de-facto for Room Acoustic simulation. Their underlying assumption – that sound propagates in straight lines, meaning sound fields may be predicted through geometrical constructions, e.g. via raytracing – leads to fast & efficient computation. But a weakness is that they do not automatically include diffraction, leading to inaccurate prediction of sound levels in some locations and unrealistic discontinuities.

So, where a scenario demands diffraction be included, it is typically added in via some separate process. These processes can be roughly grouped into three categories:

i) High precision methods for early reflections e.g. [2];
ii) Approximate and heuristic methods for late-time raytracing, typically involving ray redirection or diffraction-informed scattering coefficients;
iii) Case-specific empirical methods that detect certain conditions and add diffracted energy when present, e.g., behind obstructions such as noise barriers.

Category 1 methods are most accurate and are typically derived from full solutions to the acoustic linear wave equation and operate on pressure (with phase), so are most suited for use with algorithms such as the Image Source Method that can also compute these quantities.

But applying these methods to higher-order (repeated) diffraction – as occurs often in reality – is challenging and incurs high computational cost (though [3] and [4] propose frameworks to manage this). Switching to diffraction models derived for infinite length edges such as the Uniform Theory of Diffraction (UTD) [5] – as is used herein – can reduce this burden subject to some loss in accuracy. Table 1 in [1] identifies a small number of methods capable of implementing this to arbitrary order, but these all achieve it such that computational cost grows exponentially with diffraction order. The recent framework in [6] also falls in this category. These methods have many benefits, but they wouldn't be able to model coupled-volume reverberation, for example. For that, an algorithm where diffraction can be added to the late-time calculation without changing the order of the computational cost beyond linear is required.

An emerging category of models is what Savioja and Svensson termed "Surface-Based" GA (SBGA). These discretise the distribution of acoustic power flow versus position using a boundary mesh, just like the Boundary Element Method (BEM) uses for low frequency models. Indeed, it has been called "Energy-Intensity BEM" by some authors, but a geometrical propagator is still used, hence 'GA'. The energy distribution is discretised vs. boundary position and arrival / departure angle, as illustrated in Fig. 1 for sources, receivers and edge pairs.

Corresponding author: j.a.hargreaves@salford.ac.uk

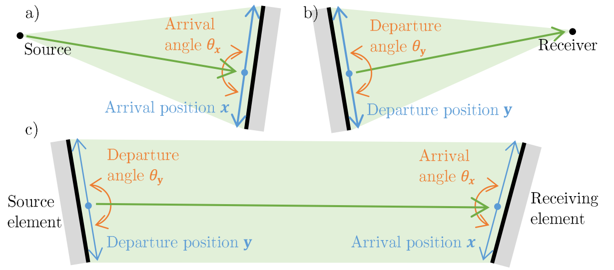

Figure 1. The three acoustic energy propagation operations in a SBGA algorithm; a) source to boundary, b) boundary to receiver, c) boundary to boundary.

Several groups have worked independently on this idea, but implementations vary (in how arrival & departure angle are parametrised especially). For a short review and an attempt to define a unifying framework see [7]. Recent work has demonstrated the power and unique capabilities of SBGA, notably for analysing coupled volumes with multi-slope reverberation decays [8].

Post-discretisation, the boundary energy distributions are represented by vectors of coefficients and the propagation operations by matrix multiplications. This leads to an algorithm structure with computational cost that scales linearly with reflection order regardless of the complexity of the constituent propagation and scattering operations. Steady state can also be solved in one step via a Neumann series. In other words, if diffraction can be added then it won't change the cost scaling since its effect will be captured in the predefined discretisation scheme instead of generating more terms.

This paper outlines an approach for adding diffraction into the SGBA framework. We note that a similar goal was pursued in [9] but believe the approach herein is better founded, being derived from the UTD [5] and placed in a framework with synergy to BEM [10]. Section 2 first presents how the UTD wedge diffraction model can be embedded into SGBA, then section 3 considers how to treat the (problematic) transition region. Conclusions and future outlook are given in 4.

Note that although this paper considers 2D wedge diffraction (Fig. 2b) it can be readily extended to 3D via a concept of a 'Keller cone' (Fig. 2c), which is the geometrical equivalent of 2.5D BEM modelling [11].

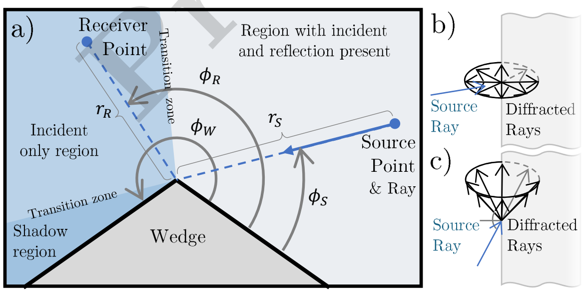

Figure 2. a) Cross-section of wedge geometry, defining angles and regions; b) 2D diffraction, as considered herein; c) Extension to 3D diffraction via a Keller cone.

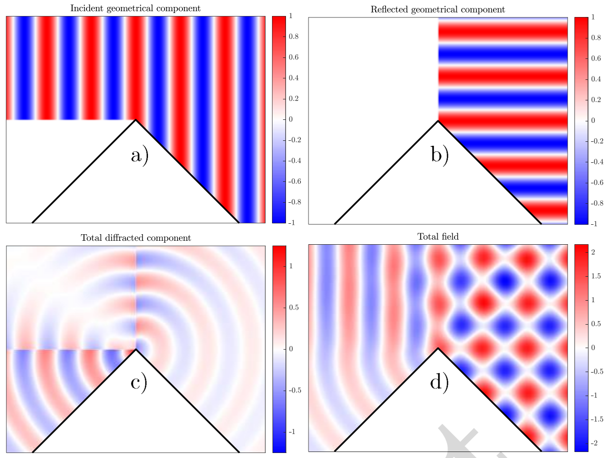

Figure 3. Real part of pressure fields predicted by the UTD wedge diffraction model for a 400Hz plane wave with $\phi_W = {}^{3\pi}/_2$ and $\phi_S = {}^{\pi}/_4$ for a domain 3m wide × 2m high: a) incident geometric component; b) reflected geometric component; c) diffracted component; d) total (=a+b+c).

2. UTD Wedge Diffraction and its inclusion into the SBGA framework

The geometry for the canonical wedge diffraction problem is presented in Fig. 2a[1]. There is insufficient space herein to fully describe this model; for this see [7] and/or [12]. An example result is shown in Fig 3.

The key point to observe[2] from Fig. 3 is that all fields are continuous and well-behaved except at the transition regions where the geometrical and diffracted fields are discontinuous. This discontinuity – while oft discussed as an intrinsic feature – is, in fact, an artefact of the 'geometric + diffraction' decomposition and doesn't occur in reality. Notably, the total field (d) is free from discontinuities because they cancel. This aids modelling of the total field efficiently in SBGA and bypasses concerns around discontinuities intersecting receiving elements. But geometric & diffracted terms must be summed as pressure in the transition zone before conversion to energy (addressed in section 3).

Focussing on the diffracted component (Fig. 3c) that needs to be added to SBGA, and ignoring the transition region temporarily, the diffracted pressure is found by:

$$P_{\text{diff}}(r_\text{R}, \phi_\text{R}) = \frac{e^{ikr_\text{S}}}{\sqrt{r_\text{S}}} D(\phi_\text{S}, \phi_\text{R}, \phi_\text{W}) \frac{e^{ikr_\text{R}}}{\sqrt{r_\text{R}}} \tag{1}$$

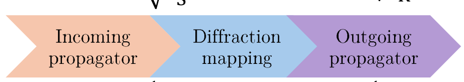

$$E_{\text{diff}}(r_\text{R}, \phi_\text{R}) = \frac{1}{r_\text{S}} |D(\phi_\text{S}, \phi_\text{R}, \phi_\text{W})|^2 \frac{1}{r_\text{R}} \tag{2}$$

1. *Note that the point source case (depicted) can be converted to plane wave scattering (shown in Fig. 3) by letting $r_S \to \infty$ and setting the incident pressure amplitude to a constant value.*
2. *The checkered pattern on the right of Fig. 3d is due to interference between the incident and reflected waves. This is a feature that an energy method intended for frequency-band averaged late-time sound energy would not be required to capture (see next section).*

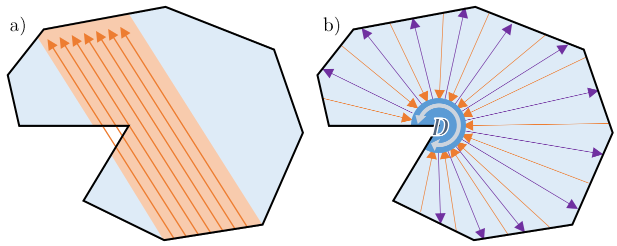

Figure 4. A polygonal domain with a wedge inclusion: a) Direct sound energy leaving a boundary patch at a given angle (representing existing SBGA approaches), where correction would be required for partial shadowing by the wedge; b) Figurative representation of the structure of Eqs. 1-7, where energy is propagated to the corner, remapped according to UTD, then propagated to receiving patches.

Equation 1 is a rewriting of Eqs. 22 and 24 from [7] where some angle-independent terms have been rolled into the diffraction directivity function $D(\phi_\mathrm{S}, \phi_\mathrm{R}, \phi_\mathrm{W})$ for brevity. Taking the magnitude-square to obtain energy, as SBGA would compute, leads to Eq. 2. Both equations have the form of concatenation of:

i) An incoming ray propagator across the domain;
ii) A diffraction-based redirection map at the corner;
iii) An outgoing ray propagator across the domain.

This process is depicted figuratively in Fig. 4b. Notably, all incoming and outgoing rays – and the angles they depart from / arrive at other boundaries – can be deduced geometrically since they connect to the corner point. It also suggests that it would be most efficient to collect them there via a discretisation scheme over angle, apply the diffraction map, and then re-radiate. This map is found by considering the middle term in eq. 2 and summing over all possible incident angles:

$$E_\mathrm{out}(\phi_\mathrm{R}) = \int_0^{\phi_\mathrm{W}} |D(\phi_\mathrm{S}, \phi_\mathrm{R}, \phi_\mathrm{W})|^2 E_\mathrm{in}(\phi_\mathrm{S}) \qquad (3)$$

The energy distributions $E_{\{\mathrm{in,out}\}}$ arriving at the corner can be efficiently represented as sums of functions that are orthogonal over $0 \leq \phi_{\{\mathrm{S,R}\}} \leq \phi_\mathrm{W}$, e.g.:

$$E_{\{\mathrm{in,out}\}}(\phi) = \sum_{n=0}^{\infty} \mathbf{e}_{\{\mathrm{in,out}\}}[n]\, P_n\left(\frac{2\phi_{\{\mathrm{S,R}\}}}{\phi_\mathrm{W}} - 1\right) \qquad (4)$$

Here P_n are Legendre polynomials and $\mathbf{e}_{\{\mathrm{in,out}\}}$ are vectors of coefficients representing $E_{\{\mathrm{in,out}\}}$. Eq. 3 can then be written as $\mathbf{e}_\mathrm{out} = \mathbf{D}\mathbf{e}_\mathrm{in}$, where:

$$\mathbf{D}[m,n] = \frac{1}{\phi_\mathrm{W}^2} \frac{2}{(2n+1)} \int_0^{\phi_\mathrm{W}} P_m\left(\frac{2\phi_\mathrm{R}}{\phi_\mathrm{W}} - 1\right) \times \int_0^{\phi_\mathrm{W}} |D(\phi_\mathrm{S}, \phi_\mathrm{R}, \phi_\mathrm{W})|^2 P_n\left(\frac{2\phi_\mathrm{S}}{\phi_\mathrm{W}} - 1\right) d\phi_\mathrm{S}\, d\phi_\mathrm{R} \qquad (5)$$

Thus, the diffraction process has been rewritten as a matrix multiplication. Similar would be done for the propagation operators from other boundaries to the corner by adapting the definitions in [7].

These steps fit neatly into the SBGA framework in [7], in which incoming and outgoing energies $E_{\{\mathrm{in,out}\}}$ at boundaries are already both discretised and scattering is handled via a Bidirectional Reflectance Density Function (BRDF) that is discretised and implemented as a matrix multiplication in a similar way. Thus, incorporating diffraction would just be a case of adding some Degrees of Freedom (DOFs) and propagation and scattering matrix blocks into the algorithm framework.

This is an attractively simple & elegant approach. The main caveat is that the relative phase of the diffracted wave is not captured due to it being an energy method (this same limitation applies to all ray-based energetic models of diffraction) and that the transition zone behaviour is not accurately captured by eq. 1. Thus, the transition zone must be handled separately, as the following section investigates.

3. The Transition Region

When casting the UTD model in Fig. 3 in a SBGA framework, it is important to realise the incident field arrives from a distant boundary (not shown) whereas the reflected field emanates from the illuminated side of the wedge. In SBGA, this reflection would be discretised separately, so the diffraction it produces in the transition region must be split in the same way so it can be combined correctly with the direct sound propagator. This is possible because the full UTD statement (Eq. 25 in [5]) contains four terms – two associated with the incident field discontinuity and two with the reflected field discontinuity – and these can be separated. The result is the pressure fields depicted in Fig. 5; note the sum of these is still equal to Fig. 3d.

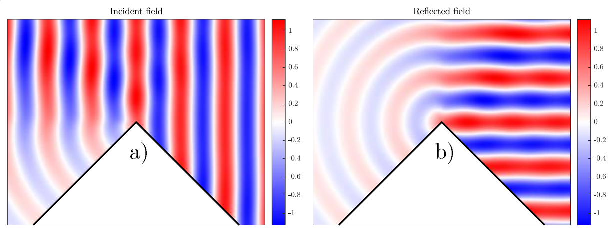

Figure 5. As Fig. 3, but with diffracted component split into two terms that make the incident (a) and reflected (b) field continuous. The sum of these still equals Fig. 3d.

Displaying pressure is intuitive and is the quantity that UTD predicts, but it is not ideal when considering its incorporation into SBGA, which models energy. Hence, Fig. 6 instead displays data as pressure magnitude squared, as is proportional to acoustic potential energy. In these, frequency has also been raised to 2kHz, a more realistic target band for SBGA usage than 400Hz.

The left column of Fig. 6 displays the raw 2kHz data from the UTD model; this is diffraction of a pure tone. The diffraction transition zone is now much narrower and clearer due to the 5× shorter wavelength, but interference effects are still evident. In Fig. 6a&c, these are between the geometric and diffracted components of each wave. In e, they're between incident & reflected.

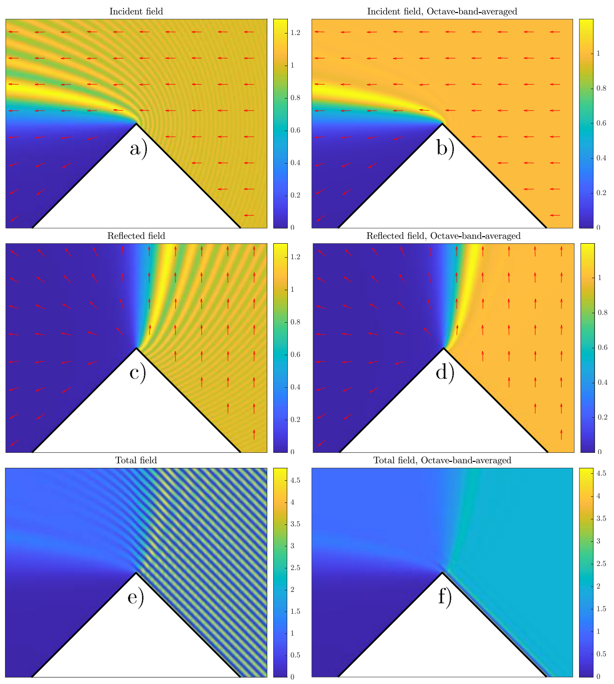

Figure 6. As Fig. 3 and 5 but plotting $|p|^2$ and with frequency increased to 2kHz. Top row is the same quantity as Fig. 5a, middle row as Fig. 5b, and bottom row as Fig. 3d. Left column is for a 2kHz pure tone. Right column is the same data averaged over the 2kHz octave band. For subplots a-d the red arrows show propagation direction, computed from the normalised active acoustic intensity.

Such interference effects are inevitable in pure tone soundfields, where all locations are coherent by definition. But they are not relevant in reverberant broadband soundfields, where the differing wavelength between – even only slightly separated frequencies – shifts the interference patterns causing them to average to zero. This is demonstrated in the righthand column of Fig. 6, where the corresponding quantities from the lefthand column have been averaged over the 2kHz octave band. The only remnants of inteference post-averaging are in locations where the formulation maintains a fixed phase relationship betweem the waves being combined. For the incident and reflected waves in Fig. 6b&d, this occurs around the transition zone. For the total field in Fig. 6f it additionally occurs near the reflecting face of the wedge where the reflected wave is in-phase with the incident wave.

But even these reduced effects wouldn't be expected in an energy-based model such as SGBA that is fundamentally incoherent, so it is desirable to remove them. But performing octave-band averaging of single-frequency models at high frequencies is time-consuming, so the data in the righthand column of Fig. 6 can't directly be used in a diffraction model for SBGA. Instead, it would be preferable to define a modification to the centre-frequency UTD result. A suggestion for how this might be achieved is presented in Fig. 7. Assessing how this compares with other more established formulations is future work but it is used to generate the SBGA illustrations that follow.

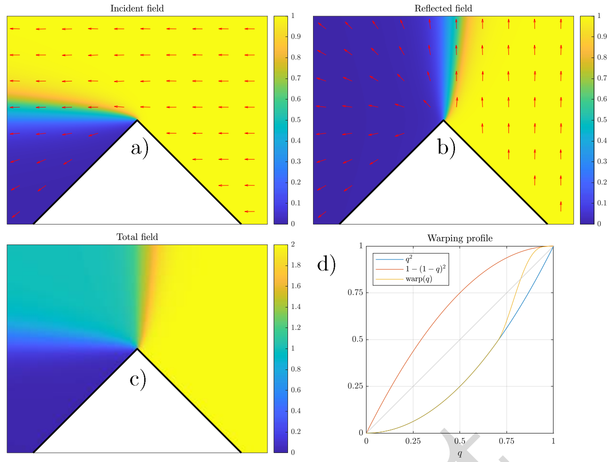

Figure 7. As Fig. 6 but approximating the octave-band averaged result by passing the energies from the individual terms in the UTD centre-frequency model separately through the warping profile in (d) and then summing.

3.1 Visualisation of Terms in an SBGA Scheme

Figure 8 shows the modified UTD energy model from Fig. 7 as it would appear as terms in a SBGA model. Note that these are plotted for a single incidence direction, whereas the way SBGA is formulated means a distribution of directions is always present.

Panels a-e show beams comprising the incident wave, as if arriving from an imagined source or boundary beyond the right extent of the plotting area, and panel f shows its diffraction. The beams in panels a, b, d and e all carry the geometric incident wave.

But the beam in panel c is different. This intercepts the wedge corner so the beam has instead been made to carry the modified transition zone UTD model on towards whatever boundary it might meet beyond the leftward extent of the plotting area. Doing this means the SBGA model can correctly calculate the soundfield through that region, which it wouldn't otherwise be capable of doing since the UTD model here requires 'with-phase' pressure summation.

Panel f shows the diffracted energy alone, as would be handled according to Eqs. 3-5. As plotted, this still shows the energy heading through the transition zone, but in an SBGA implementation this would need to be nullified for the next patch the beam in panel c hit, to avoid counting that energy twice.

Panels g-j show similar for the reflected wave, which originates from the illuminated side of the wedge in response to the incoming beams in panels a-e. The beams in panels h and i are purely geometric, but the one in panel g – which intercepts the wedge corner – again propagates the modified UTD transition zone model. Panel j shows the diffraction alone, which again would need to be nullified for any patch that the beam in panel g hit. The strength of this term would be dictated by the strength of the outgoing wave at the wedge tip (the beam in panel g again).

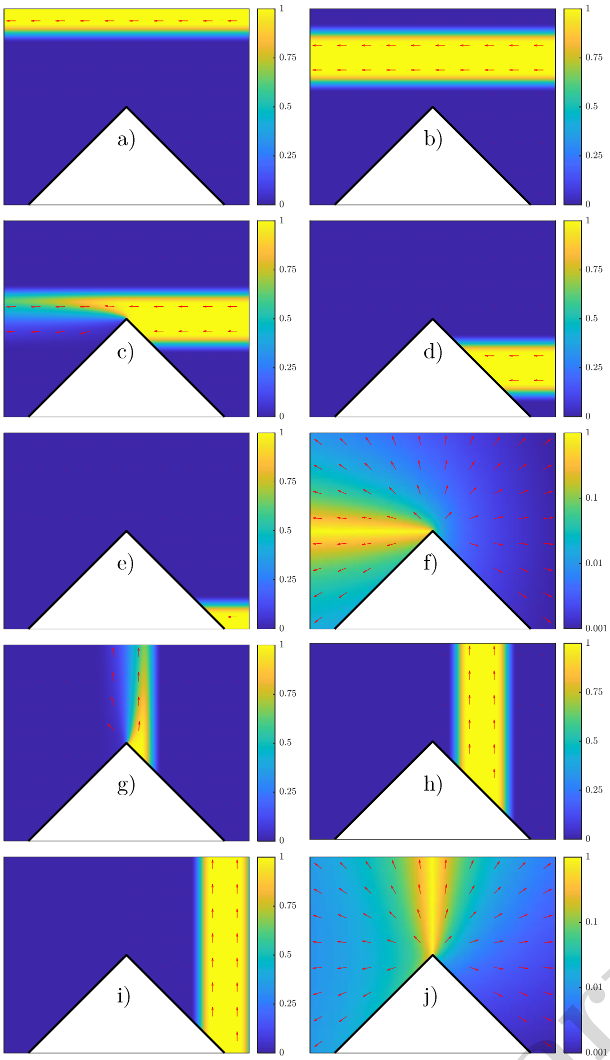

Figure 8. Visualisation of how the modified UTD energy model in Fig. 7 would appear as terms in an SBGA model. Panels a-e show beams comprising the incident wave, and panel f its diffraction. Panels g-i show beams comprising the reflected wave, and panel j its diffraction. Note that the diffraction terms have a logarithmic colour scale to better show their extent.

4. Conclusions & Future Outlook

An approach to integrate and efficiently represent the Uniform Theory of Diffraction (UTD) in a Surface Based Geometrical Acoustics (SBGA) algorithm has been presented. Key conclusions are that:

- SBGA is highly suitable for late-time reverberant sound fields, having computational cost that scales linearly with reflection order even when complex boundary scattering occurs, and a means for solving for steady state in one step. Moreover, multi-slope coupled volume decays can be analysed [8].

- SBGA also very suitable – in principle – for incorporating diffraction since it can be captured accurately with a controlled number of Degrees Of Freedom (DOFs). This is in contrast to raytracing models of diffraction, where an explosion of extra rays is required to achieve accuracy.

- This can be very efficiently done by adding a small number of extra DOFs at the diffracting edge to discretise the incoming and outgoing diffracted field.

- But modelling of the transition zone requires special treatment since 'with-phase' summing of geometrical and diffracted pressure is required here. This is done separately for the incident and reflection waves because SBGA would handle them separately.

Limitations of the presented approach are that a special case is required for the transition zone – it would be more elegant if it weren't – but avoiding this would need a variant of SBGA that tracked phased pressure to be developed. This is not impossible – ref. [10] discusses such ideas – but is unlikely to be suitable for late-time modelling, as has been the motivation here.

Future work is to integrate the presented approach into a full SBGA codebase; it is anticipated that this would be most readily done first in 2D – which would test the principles – and then extended to 3D (which is more complicated geometrically and computationally costly). Finally, integration into a full-audible bandwidth unified simulation framework as described in [10] and production of auralisation remains the ultimate goal.

References

[1] L. Savioja and U. P. Svensson: "Overview of geometrical room acoustic modeling techniques," *J. Acoust. Soc. Am.,* vol. 138, no. 2, pp. 708–730 2015.

[2] U. P. Svensson, R. I. Fred, and J. Vanderkooy: "An analytic secondary source model of edge diffraction impulse responses," *J. Acoust. Soc. Am.*, vol. 106, no. 5, pp. 2331–2344, 1999.

[3] A. Asheim and U. P. Svensson, "An integral equation formulation for the diffraction from convex plates and polyhedral," *J. Acoust. Soc. Am.*, vol. 133, no. 6, pp. 3681–91, 2013.

[4] M. W. Ospel, "Iterative path expansion for Helmholtz scattering with Neumann boundary conditions," *J. Acoust. Soc. Am.*, vol. 159, no. 1, pp. 600–609, 2026.

[5] R. G. Kouyoumjian and P. H. Pathak, "A uniform geometrical theory of diffraction for an edge in a perfectly conducting surface," *Proceedings of the IEEE*, vol. 62, no. 11, pp. 1448–1461, 1974.

[6] P. Palenda and M. Vorländer, "Auralizing arbitrary urban environments including diffraction," *Acta Acustica*, vol. 10, p. 46, 2026.

[7] A. Emthyas and J. Hargreaves, "Raytracing in Galerkin Boundary Integral form," *Proc. InterNoise 22*, Glasgow, UK, August 2023, doi: 10.3397/IN_2022_0345.

[8] M. Scerbo, S. J. Schlecht, R. Ali, L. Savioja, and E. De Sena, "Modeling Nonuniform Energy Decay Through the Modal Decomposition of Acoustic Radiance Transfer," *IEEE Trans. Audio Speech Lang. Process.*, vol. 33, pp. 3363–3376, 2025.

[9] A. Pohl and U. M. Stephenson, "A Combination of the Sound Particle Simulation Method and the Radiosity Method," *Building Acoustics*, vol. 18, no. 1, pp. 97–122, 2011.

[10] J. Hargreaves, "A comparison between the high-frequency Boundary Element Method and Surface-Based Geometrical Acoustics," *Proc. InterNoise 22*, Glasgow, UK, August 2023, doi: 10.3397/IN_2022_1005.

[11] A. D. Pierce, Acoustics - An Introduction to Its Physical Principles and Applications, 3rd ed. Springer International Publishing, 2019.

[12] T. Sakuma, S. Sakamoto, and T. Otsuru, Computational Simulation in Architectural and Environmental Acoustics. Springer Japan, 2014.